BOREAL ENVIRONMENT RESEARCH 30: 39–54
ISSN 1797-2469 (online)

Helsinki 29 January 2025

# Carex Model: A Mire Microtopography Formation Model using Numerical Simulation

Misao Okada[1)2)*] and Takashi Inoue[3)]

[1)] *Okadax Technology Engineering Inc., Sapporo., Japan*
[2)] *Suiko Research Co., Ltd., Sapporo, Japan*
[3)] *Research Faculty of Agriculture, Hokkaido University, Sapporo, Japan*
**corresponding author's e-mail: okadax@suiko-r.co.jp or okadax@sage.ocn.ne.jp*

*Received 6 Nov. 2023, final version received 29 Oct. 2024, accepted 8 Nov. 2024*

Okada M. & Inoue T. 2025: Carex Model: A Mire Microtopography Formation Model using Numerical Simulation. *Boreal Env. Res.* 30: 39–54.

Boreal mires have various microtopographies with patterns that sometimes present mysterious shapes not seen elsewhere. Having studied these interesting microtopographical patterns that exist in Japanese mountainous mires, we developed an original computer simulation model named "Carex" to help understand the mechanism of their formation processes. The basic premise of this model is that water table fluctuations due to precipitation affect the amount of peat accumulation, which in turn causes changes in mire microtopography. The Carex model is a simple physical model with clear plant ecological causal relationships and realistic spatiotemporal scales, suitable for understanding the mechanisms of mire pattern formation. Application of the model provided convincing explanations for the formation processes of some typical microtopographical patterns. In this paper, we describe the concept and basic structure of the Carex model.

## Introduction

Mires exhibit a variety of microtopographical patterns that correspond to their environment, and they often have mysterious shapes not seen elsewhere. Consequently, they have long attracted the interest of researchers and have been the subject of active research. With the development of computing technology, some researchers have tried to understand the mechanisms of mire pattern formation using computer simulation models.

Swanson and Grigal (1988) originally constructed such models of mire patterning. They were able to reproduce a string pattern by determining the probability of hummock occurrence in relation to the water table. However, their model had the problem that the patterns moved downstream on the slope over time. The reason was that they used a linear function to express the relationship between the water table and hummock formation probability, such that the hummock formation probability increased unilaterally as the water table lowered. On the upstream side of a hummock, the water table tends to rise and thus the hummock formation probability decreases. Conversely, on the downstream side, the water table is lower and thus the hummock formation probability increases. Consequently, the hummock appears to move in the downstream direction of the slope over time. Couwenberg (2005) revisited this model, partially correcting it to show that patterns anatomose and merge. Couwenberg and Joosten

*Editor in charge of this article: Christina Biasi*
https://doi.org/10.58013/ber2025.7amd-7m45

(2005) applied the model to a raised bog and showed how small-scale processes can create a variety of large landscape patterns. However, they also encountered the same problem of the pattern moving downward on the slope because they used the same linear function as Swanson and Grigal (1988).

Alexandrov (1988: fig. 3-2) believed that the rate of peat accumulation is determined only by hydrologic factors, supposing complete correspondence between the vegetation distribution and the bog water level and throughflow. Using a hydrologic model, it was concluded that it is acceptable to consider only the effect of the bog water level on the local rate of peat accumulation.

Belyea and Clymo (2001) presented a feedback mechanism of steady rates of peat formation over the long term. In their analysis, they used four equations: productivity, rate of decay, dry bulk density, and rate of peat formation, adopting the acrotelm thickness as the independent variable. Using the relationship between the rate of peat formation and water table depth, they explained the stability of the long-term rate of peat formation. Rietkerk *et al*. (2004) proposed that the patterns are self-organized and originate via a nutrient accumulation mechanism. They expressed the interaction between the vascular plant biomass, hydraulic head, and nutrient availability using three partial differential equation systems, and determined the spatial distributions of plant biomass. Subsequently, they reproduced string patterns on slopes and maze patterns on flat ground. Eppinga *et al*. (2009) presented a model that described spatial interactions between four mechanisms. They used the model to study pattern formation driven by three different mechanisms: peat accumulation, water ponding, and nutrient accumulation. Through on-and-off switching of each mechanism, they showed how these mechanisms affect surface patterning. However, the very complex equations expressing the basic mechanisms make it difficult to understand the contribution of each parameter. Moreover, there is concern that arbitrary operations might be involved in determining the parameters. To develop a universal model, we believe that the number of parameters should be reduced as much as possible and that the mechanism should be expressed more simply.

Harris *et al*. (2020) suggested that the development of distinct microtopographies is dependent on the ecohydrological setting, which in turn influences the processes controlling peat accumulation at the microform scale in their conceptual model. They also suggested that the strength and direction of feedbacks among the vegetation and the hydrology differ between sites with varying ecohydrological conditions. For example, the relationship of gross primary productivity to water table depth in a bog is negative, meaning that an area with a deeper water table has lower gross primary productivity.

Many of the above models consider changes in microtopographical patterns related to water levels. However, some models lack stability owing to their use of linear parametric functions, while others ignore surface water movement. Moreover, certain models cannot be applied to existing mires because the spatiotemporal scales are unclear. Independently of the above models, Okada (2008) proposed the "Carex" model to determine the formation process of microtopographical patterns observed in Japanese mires. In this model, surface water movement is treated as important as groundwater movement for reasons that are described later. The Carex model was developed by considering the environmental conditions of mountainous wet mires in which natural hydraulic conditions are well preserved. In mountainous areas of Japan, not only is it rainy in summer but there is also much snowfall in winter, and the snow depth can reach several meters. The snowmelt period sometimes extends into June and the first snow falls in October. These events are repeated annually and the accumulated peat is strongly compacted by the weight of the snow, which greatly affects water permeability. During the short snow-free period, plants grow under the influence of the ambient environmental conditions and dead plant material accumulates on the upper peat layer.

As described by Lindsay (2010), "peat bog soils are a direct product of vegetation growth," and the formation of mire microtopographies depends on the accumulation rate of peat deposits. The amount of primary production of vegetation (PPV) therefore dominates the development

of microtopographies under various environmental conditions. The Carex model is intended to quantify the process via which microtopographies on a horizontal scale of several meters change gradually under various environmental conditions. The relevant events occur in the following order: initial rainfall, water movement, water table fluctuation, and plant growth. Depending on the environmental conditions, PPV will vary spatially and peat will accumulate accordingly. The slight differences in the rate of peat accumulation make the peat surface uneven and eventually cause the topography to changes. Therefore, we coded the Carex simulation program to realize just such a scenario.

Unlike previous models, the Carex model assumes that water moves along the topographic shape of a mire at a realistic spatial scale. Under these conditions, vegetation grows and withers, and ultimately accumulates as peat, and the topography changes with the amount of peat accumulation. Using the water table, the Carex model combines the physical phenomenon of water movement in mires with the ecological factor of plant growth characteristics. Therefore, it can be classified as a dynamic eco-physical or physico-ecological model.

To a large extent, PPV depends on the water table in mires (Hogetsu *et al*. 1954; see also Nungesser 2003; Swanson 2007), and the peat accumulation rate in Japan, after subtracting decomposition, is approximately 1 mm $y^{-1}$ (e.g., Hirakawa 2002, Kito and Hotes 2014). On the basis of these relationships, Okada (2008) created a peat growth function (PGF) that links the peat accumulation rate to water table fluctuation during the plant growth period, assuming that this rate is proportional to PPV.

The Carex model uses the water table as the only parameter to quantify the PPV amount using the above relationships. Rainfall and its subsequent movement as surface water affect water table fluctuation, and the model places equal emphasis on the influence of surface water flow and groundwater in application to the humid environment of Japan. The frequency of occurrence of surface water flow on mires is low, but surface water moves more rapidly than groundwater and is strongly influenced by the irregularities of the uneven surface. Therefore, surface water flow has substantial impact on the distribution of water over mires. A slight difference in surface irregularities affects the movement of surface water and influences the water table.

Differences in the water table lead to variations in vegetation growth, which determine the amount of peat accumulation. Therefore, because the movement of surface water is very important, the Carex model deals with surface water flow in detail.

Several of the existing simulation models introduced above ignore surface water flow or substitute Darcy's law in their calculations. Because Darcy's law was developed to express the frictional resistance of pipe flow, we believe that it is unsuitable for quantifying the movement of surface water. The Carex model uses Darcy's law to calculate the groundwater flow and uses Manning's law for calculating the surface water flow. Because surface water moves rapidly, the calculation time interval must be shortened appropriately to ensure the calculative stability of Manning's law, which means that the model requires a long calculation time. However, we developed the model because it has the advantage of quantifying detailed topographic change.

## Methods

### Basic equations of water movement in mires

In the model, it is first necessary to determine how water flows under given boundary conditions. Specifically, surface water and groundwater flow simultaneously in the mires. Furthermore, because the two flows are interdependent, it is important to understand both.
The primitive equations of unsteady flow of the surface water and groundwater are shown below. The meaning of the symbols is given in (Fig. 1).

a) Surface water flow (unsteady state)

The governing equations of surface water flow are as follows:

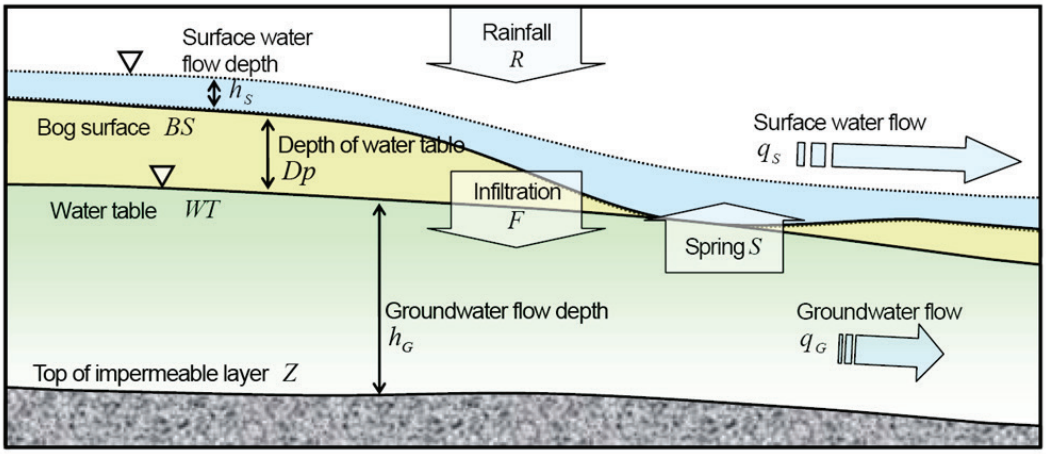


**Fig 1.** Schematic profile of water flow in a mire. Water reaches the ground surface as rainfall infiltrates underground according to Horton's infiltration equation, and remaining water is added to surface water. Depending on the topography and shape of the water surface, the surface flow and groundwater flow will move downstream while infiltrating the ground and emerging via springs.

[Equation of continuity]:

$$\frac{\partial h_S}{\partial t} + \frac{\partial q_{Sx}}{\partial x} + \frac{\partial q_{Sy}}{\partial y} = R - F + S. \tag{1}$$

[Equation of motion in $x$-direction]

$$\frac{\partial q_{Sx}}{\partial t} + \frac{\partial u_x q_{Sx}}{\partial x} + \frac{\partial u_y q_{Sx}}{\partial y} = -gh_S \frac{\partial (h_S + BS)}{\partial x} - gn^2 \frac{q_{Sx}\sqrt{u_x^2 + u_y^2}}{h_S^{4/3}}. \tag{2}$$

[Equation of motion in $y$-direction]

$$\frac{\partial q_{Sy}}{\partial t} + \frac{\partial u_x q_{Sy}}{\partial x} + \frac{\partial u_y q_{Sy}}{\partial y} = -gh_S \frac{\partial (h_S + BS)}{\partial y} - gn^2 \frac{q_{Sy}\sqrt{u_x^2 + u_y^2}}{h_S^{4/3}}, \tag{3}$$

where $x$ and $y$ are fixed horizontal coordinates, $t$ is time (s), $h_S$ is depth of the surface water flow (m), $q_{Sx}$ and $q_{Sy}$ are surface water flow discharges per unit width in the $x$ and $y$ directions (m$^2$ s$^{-1}$), respectively, $R$ is rainfall intensity (m s$^{-1}$), $F$ is infiltration intensity (m s$^{-1}$), and $S$ is the spring flow intensity (m s$^{-1}$). In Eqs. 2 and 3, $u_x$ and $u_y$ are speeds of the surface water flow in the $x$ and $y$ directions (m s$^{-1}$), $g$ is acceleration due to gravity (m s$^{-2}$), $n$ is the roughness coefficient in Manning's formula (e.g., Chow 1959), and $BS$ is the elevation of a bog surface (m).

b) Infiltration

Infiltration intensity $F$ is expressed by Horton's infiltration equation (Horton, 1940):

$$F = f_c + (f_0 - f_c)\exp(-\alpha t), \tag{4}$$

where $f_c$ is the final infiltration intensity (m s$^{-1}$) and $f_0$ the initial infiltration intensity (m s$^{-1}$). $\alpha = (\ln 2) / T$ is a constant, with $T$ denoting the time over which infiltration intensity declines by half.

c) Unconfined groundwater flow (unsteady state)

The equation of continuity of unconfined groundwater flow is expressed by Eq. 5, and the equations of motion of that groundwater are expressed by Eqs. 6 and 7 using Darcy's law (e.g., Whitaker, 1986) based on the Dupuit-Forchheimer's assumption. That assumption is that the water head gradient is small and groundwater flow velocity is constant with depth.

[Equation of continuity]

$$\lambda_e \frac{\partial h_G}{\partial t} + \frac{\partial q_{G_x}}{\partial x} + \frac{\partial q_{G_y}}{\partial y} = F - S. \tag{5}$$

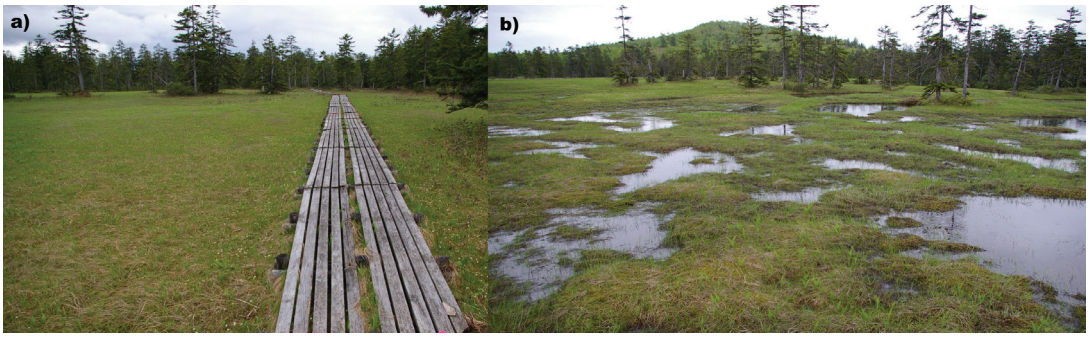


**Fig 2.** (**a**) Grassland-like flat mire surface (Ukishima-mire, Hokkaido, Japan; 43°55′53.10′′N, 142°57′33.83′′E) and (**b**) micro-relief of hummocks and shallow hollows (Ukishima-mire, Hokkaido, Japan; 43°55′56.92′′N, 142°57′35.64′′E).

[Equation of motion in $x$-direction]

$$q_{Gx} = -k_x h_G \frac{\partial (h_G + Z)}{\partial x}. \quad (6)$$

[Equation of motion in $y$-direction]

$$q_{Gy} = -k_y h_G \frac{\partial (h_G + Z)}{\partial y}. \quad (7)$$

Here, $h_G$ is the depth of unconfined groundwater flow (m), $q_{Gx}$ and $q_{Gy}$ are groundwater flow discharges per unit width in the $x$ and $y$ directions ($m^2\ s^{-1}$), $\lambda_e$ is effective porosity, $k_x$ and $k_y$ are the coefficients of permeability in the $x$ and $y$ directions ($m\ s^{-1}$), and Z is elevation of the impermeable layer (m).

In the calculation, we used the leapfrog method (e.g., Fornberg 1973), which is a type of finite differencing. In the first half-step, discharges per unit width $q_{Sx}$, $q_{Sy}$ , $q_{Gx}$ and $q_{Gy}$ are calculated by the equations of motion (Eqs. 2, 3, 6 and 7), and in the latter half-step, water depths $h_S$ and $h_G$ are defined by the equations of continuity (Eqs. 1 and 5). When there is surface water flow, for calculative stability, the time interval $\Delta t$ must satisfy the following equation, with $\Delta x$ being the spatial difference interval.

$$\Delta t < \Delta x / \sqrt{g h_s}. \quad (8)$$

For satisfying the calculative stability condition (Eq. 8), $\Delta t$ must be shortened as the depth $h_s$ of the pond in the mire increases. As a result, the number of calculation steps increases and the calculation period lengthens. If $\Delta x$ between the grids dividing the calculation area is halved, the number of calculation steps double and the number of grids to be calculated quadruples, so the time required for calculation is increased by eight. Therefore, it is necessary to balance the required calculation accuracy with the calculation time.

## Peat growth function

Various factors of mires influence PPV. Nungesser (2003) identified temperature, solar radiation, pH, and the water table as having an impact on net PPV. Among those factors, the water table is the only one that can change over a horizontal scale of several meters. Therefore, in the model, we considered it appropriate that PPV be quantified in relation to the water table rather than to any other factor.

In mires, there are areas of flat grassland (Fig. 2a; 43°55′53.10′′N, 142°57′33.83′′E) and uneven areas of irregular ridges and hollows with waterlogged depressions (Fig. 2b; 43°55′56.92′′N, 142°57′35.64′′E), and differences exist in the hydrologic conditions between those two types of landscapes. As explained later, a flat surface can develop under certain conditions, whereas an uneven surface can form under other conditions. To predict PPV, the relationship between vegetation growth and the water table must reflect the differences in the boundary conditions between the two landscapes.

Hogetsu *et al*. (1954) indicated that differences in the water table have the most important

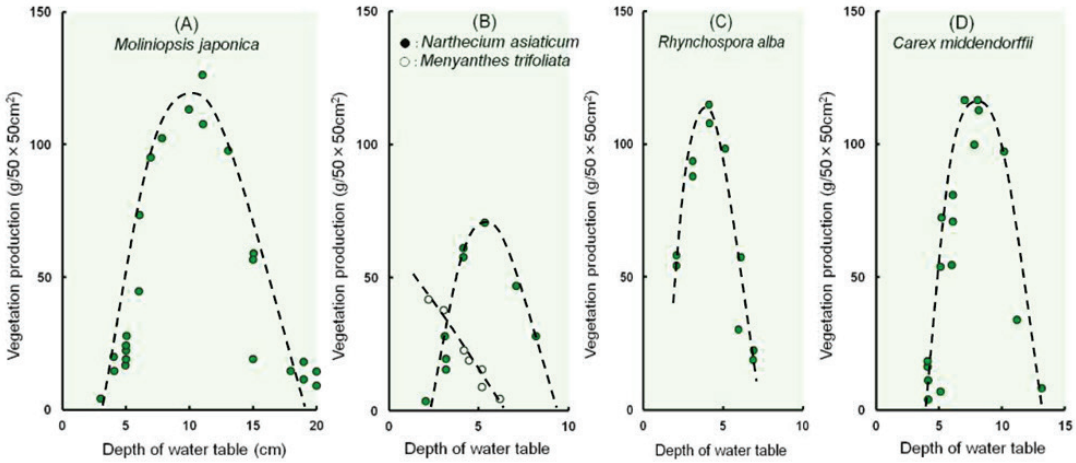


**Fig 3.** Vegetation production in relation to water table depth (partly revised from Hogetsu et al. 1954). (**A**) *Moliniopsis japonica*; (**B**) *Narthecium asiaticum* (green) *Menyanthes trifoliata* (white); (**C**) *Rhynchospora alba*; (**D**) *Carex middendorffii*. Many plant species respond to water table depths of 5-10 cm in achieving maximum primary production.

impact on the PPV in mires. They also claimed that a specific water table exists that is suitable for every plant species growing in those mires. The relationship between water table depth (horizontal axis) in an area of vegetation growth and PPV (vertical axis) is illustrated in Fig. 3 (Hogetsu *et al*. 1954). The graphs demonstrate that most plant species respond to a water table depth of 5–10 cm in achieving maximum primary production. The graphs have a shape that resembles a normal distribution, and they are very useful for determining the water table depth that leads to maximum PPV. Moreover, after subtracting decomposition, the peat accumulation rate in Japanese mountainous mires is approximately 1 mm $y^{-1}$ (e.g., Hirakawa 2002, Kito and Hotes 2014). Therefore, by combining those factors, the peat accumulation rate can be estimated based on water table fluctuation.

Vegetation grows and dies, and plant litter accumulates and becomes peat. The Carex model is built on the average growth characteristics of various plants instead of individuals, and PPV has a relationship with the fluctuating water table during the plant growth period (Fig. 3). Analogously, the accumulation of peat in mires is presumed proportional to PPV. With consideration of work by Hogetsu *et al.* (1954), Okada (2008) created a logarithmic normal distribution function (Eq. 9) as a PGF, which used the coefficient $G_{max}$ to transform PPV into the final objective peat accumulation *Gr*:

[Peat growth function]

$$Gr = G_{max} \exp\left[-\left\{\ln(b(Dp - Dc))\right\}^2\right], \quad (9)$$

where *Gr* is the peat accumulation at each location (mm $y^{-1}$), $G_{max}$ is the maximum peat accumulation rate including peat compaction and decomposition as a negative component (mm $y^{-1}$), *Dp* is the average water table depth during the plant growth period (m), *Dc* is the critical depth of the water table at which plants can grow (m), $b = 1 / (Dp_{max} - Dc)$ is a parameter of sharpness ($m^{-1}$), and $Dp_{max}$ is the water table depth yielding the maximum peat accumulation.

Parameter *Dp* is expressed by the following relationship, where *BS* is the elevation of the bog surface (m) and *WT* is the water table depth (m) (Fig. 1):

$$Dp = BS - WT. \quad (10)$$

A negative value of *Dp* means that the bog surface is waterlogged (i.e., submerged).

For example, substituting $G_{max}$ = 1.0 mm $y^{-1}$, $b$ = 10.0 $m^{-1}$, and $Dc$ = –0.05 m, *Gr* varies as illustrated in Fig. 4. When the water table depth

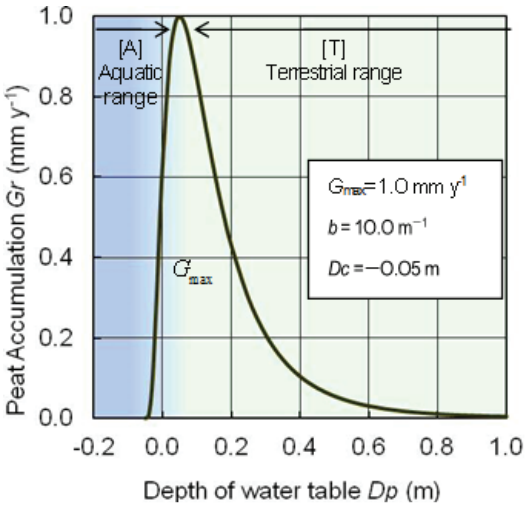


**Fig 4.** Example of peat growth function (PGF) using the lognormal distribution function. The parameters used here were determined from plant growth characteristics and peat decomposition rates. The hydraulic environment in which plants grow changes according to the growth characteristics of the plants growing there.

fluctuates mainly in the terrestrial range ([T] in Fig. 4), the shallower that depth, the greater the value of $Gr$ . Consequently, an uneven bog surface becomes flat (as pictured in Fig. 2a). In contrast, when the water level tends to fluctuate in the aquatic range ([A] in Fig. 4) and the water table depth is shallow or negative (submerged condition), the shallower the depth, the smaller the value of $Gr$ . When this condition persists for a long time, the unevenness of the mire surface becomes more remarkable (as pictured in Fig. 2b), and open water zones become permanent. The specific values given to $b$ and $Dc$ were determined based on Hogetsu *et al.* (1954), and $G_{max}$ was established based on Hirakawa (2002) or Kito and Hotes (2014).

We constructed the PGF based on several vascular plant properties shown by Hougetsu *et al*. (1954) that we adopted as an average characteristic of common vegetation. Depending on the setup, the PGF can represent certain plant growth characteristics, but we believe that the phenomenon should be simplified in the early stages of modeling. When the water table depth satisfies the relationship $Dp = Dc + 1 / b$ in the PGF, $Gr$ is maximized ($Dp = Dp_{max}$), and $Dc$ can be interpreted as a determinant of the future condition of the bog surface. If the waterlogged condition remains deeper than the critical depth over many years, peat will not accumulate. Consequently, such a site becomes an aquatic zone surrounded by areas of peat deposition.

When the parameters of Eq. 9 are determined as illustrated in Fig. 4, the water table depth of maximum vegetation growth is +5 cm and the limit of vegetation growth is –5 cm. In other words, –5 cm is the initial condition for permanent submergence.

## Results

### Initial and boundary conditions

We applied the Carex model to the mountainous mires in Japan. The Japanese archipelago has unique climatic conditions owing to its geographic location. The Sea of Japan stretches between the Japanese archipelago and the Eurasian continent, and a warm ocean current flows from the southwest toward the northeast through this sea. During winter, the monsoon winds blow from the Eurasian continent toward Japan, and water vapor supplied by the Sea of Japan falls as snow on the Japanese archipelago. In northern Japan, snowfall occurs frequently and the depth of the snow cover can exceed 1 m, even on the low-lying plains. In the mountainous areas targeted in our study, this depth can sometimes exceed several meters. In areas with such a large amount of snow in winter, peat does not freeze but is heavily loaded and compacted. Furthermore, the water table tends to remain high, even after the snow melts.

In Japan, even on the plains around prefectural capitals, precipitation ranges from 1000 to 2800 mm y$^{-1}$ (Japanese Meteorological Agency). In mountainous areas, there are insufficient observation points, but some observations indicate that the precipitation amount can be several times greater than that on the plains. Given that the climate of Japan is characterized by heavy rainfall and high humidity, even in summer, compacted peat in a natural mire often remains moist all the time. In such an environment, decomposition of peat in the mire can

occur, but the amount is small and varies little spatially. The Carex model also assumes that peat decomposition is spatially uniform and weak, and the rate of peat accumulation is taken as the PPV minus this decomposition. We set the PGF constants (Fig. 4) with consideration of the climate of Japan.

When applying the Carex model to mires in regions with a different climate or other characteristics of peat, the PGF constants should be adjusted appropriately.

The rainfall time series data that constituted the starting point for all computational processes are based on 2-hourly rainfall observed during June–October 1994 at the Sarobetsu-mire in northern Japan. Most of the mires mentioned in this paper are in mountainous areas or remote areas for which there is no meteorological information available. However, there is a meteorological observation station near the Sarobetsu-mire, which has a continuous, albeit not long-term, record of observed rainfall data. We make use of this dataset as a standard basis. Because the Sarobetsu-mire and other mires have similar environmental conditions, we concluded that they probably have similar rainfall conditions. We selected rainfall data relevant to the Sarobetsu-mire in 1994 because the total rainfall was near normal, and the rainy and dry seasons were clearly separated. The observed 2-hourly rainfall was summed for each day to obtain the daily rainfall, the value of which was proportionally divided by the time differential interval $\Delta t$ and used for subsequent calculation. On the basis of these rainfall data, we created hyetographs of heavy, light, and normal rainfall patterns as options for rainfall boundary conditions. Each rainfall pattern of 3–4 months corresponding to the plant growth period was treated as 1-year data and used repeatedly.

At the onset of rainfall, infiltration begins with initial infiltration intensity $f_0$. If the water table depth is positive, rainfall will infiltrate the groundwater at that point with an infiltration intensity given by Horton's infiltration formula (Eq. 4). When the water table depth drops below zero (i.e., when water begins to pool at the surface), rainfall is captured by the surface water. The formula is reset when the daily rainfall is zero.

In the Sarobetsu-mire where rainfall data were observed, there are no measured values for the parameters of Horton's infiltration formula. Therefore, on the basis of the measured rainfall and using the same basic equations as in the Carex model, we simulated a two-dimensional groundwater flow with combinations of various parameter values, from which we selected the combination that effectively reproduced the measured water table fluctuations. Consequently, we obtained values of $f_0$ = 40 mm h$^{-1}$, $f_c$ = 10 mm h$^{-1}$, the time over which the infiltration intensity declined by half as $T$ = 0.2 h (in Eq. 4), effective porosity $\lambda_e$ = 0.2 (in Eq. 5), Manning's roughness coefficient $n$ = 1.0 (in Eqs. 2 and 3), and coefficients of permeability $k_x$ and $k_y$ = 0.01 cm s$^{-1}$ (in Eqs. 6 and 7).

The initial value of the water table at the start of calculation was assigned as 2 cm below the surface, assuming the mire condition immediately after snowmelt. For each subsequent year, initial values for the groundwater and the surface water table were taken as the average values obtained from calculations for the previous year.

When the total rainfall cannot infiltrate into the ground and water runs off to the surface, surface water is calculated according to Manning's law. When surface depressions are submerged to form ponds, there is the risk that surface water level calculations will diverge because of wave propagation. To avoid this, $\Delta t$ must be determined such that it satisfies the stability condition of Eq. 8. The differential time interval $\Delta t$ for the boundary conditions assumed in this model was approximately 0.1–2.0 s. Therefore, calculation of one plant growth period (i.e., one year) would require 5–100 million iterations. If this were repeated for hundreds to thousands of years, the amount of calculation would be huge and take a very long time; therefore, it was necessary to devise a method to shorten this time.To shorten the calculation time without affecting the result, we verified by how much the time could be shortened by multiplying the maximum accumulation amount $G_{max}$ of the PGF in Eq. 9 by an acceleration factor (AF). The Carex model calculates annual peat growth (i.e., annual accumulation amount) at each point

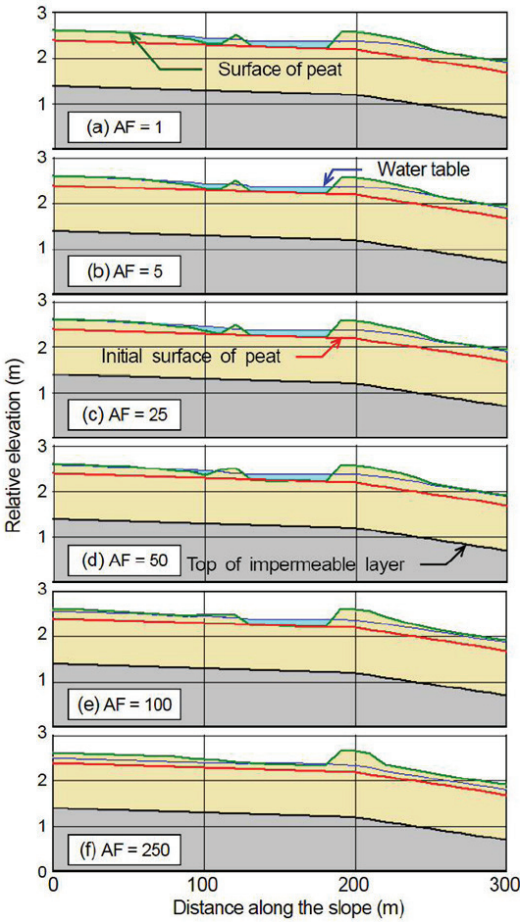


**Fig 5.** Difference in topography after 500 years formed by different values of the acceleration factor (AF).
(AF = 1): The amount of microtopographical change is calculated using the PGF based on water table fluctuations due to precipitation during the plant growth period. Then, the amount of topographical change is calculated for the changed topography using the same procedure. The results of repeating this 500 times are shown in the panel AF = 1.
(AF = 250): Similarly, calculate the amount of microtopographical change and multiply it by 250. The results of repeating this process twice are shown in the panel AF = 250.

based on the average water table at each point obtained from the hydraulic calculation for one plant growth period (i.e., one year). Furthermore, we multiplied the maximum accumulation amount by the AF to determine the peat accumulation for AF years. Comparing the results of annual peat accumulation calculations over 500 years, the results for AF = 25 were found

**Fig 6.** Ponds on the stair-like slope in Naebayama-mire. (36°50´43.03´´N, 138°41´32.47´´E; elevation: 2100 m) (Photo: Hitomi Kimura).

almost the same as those for AF = 1, and the difference for AF = 50 was practically negligible (Fig. 5). Therefore, we determined that taking AF = 10–50 would not make a difference to the results. In other words, to obtain the results after 1000 years, we shortened the calculation time by setting the plant growth period for 100 to 20.

## Application to stair-like slope

The formation processes of the microtopographies of the mires in Japan have been explained qualitatively (e.g., Yoshii and Hayashi 1935; Hori 1961); using the Carex model, a quantitative explanation can be provided. On the basis of many boreholes, Hori and Yajima (1954) and Hori (1961) acquired cross-sectional measurements of a stair-like slope with a number of ponds in the Naebayama-mire (Fig. 6). In their studies, the surface shape of the mire and the locations of the ponds were clearly identified, and the depth of the impermeable layer was also accurately indicated; therefore, we determined that this mire was suitable as an example for calculation using the Carex model. Mount Naebayama is in the central part of the Japanese archipelago (36°50´43.03´´N, 138°41´32.47´´E). The mountain is a volcano that formed approximately 300 000 years ago and it stands 2145 m above sea level. The entire summit is a gently sloping lava plateau that forms a table-like shape with surrounding cliffs. The Naebayama-mire covers approximately 600 ha of the summit of the lava plateau area. The measured elevation of

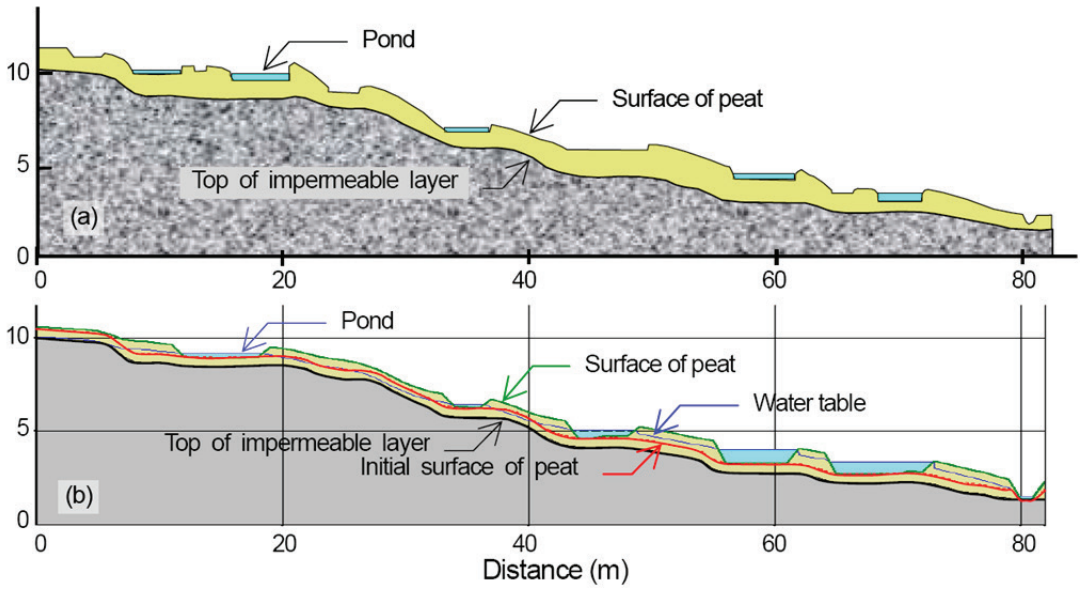


**Fig 7.** Configuration of hollows in Naebayama-mire, Nagano, Japan. (**a**) Profile measured by Hori and Yajima (1954) and (**b**) profile simulated using the one-dimensional Carex model. Green line: peat surface, Blue line: water table, Red line: Initial surface of peat, Black line: Top of impermeable layer.

the mire surface and the top of the impermeable layer are depicted in Fig. 7a. It is evident that the peat deposit thickened where the slope changed from a gentle to steep incline in the downstream direction, with a pond formed on the flat portion on the upstream side. A nearly 100-m-long section of the peatland of Mt. Naebayama shows several ponds and waterless depressions in a stair-like slope (Fig. 7a). In the calculations, the elevation of the impermeable layer depicted in Fig. 7a was used as the topographic initial condition. Because this slope is the southern slope just below the summit of Mt. Naebayama, the boundary on the left-hand side of the figure was treated as closed, and it was assumed that there was no groundwater supply from upstream.

We applied the one-dimensional Carex model to the stair-like slope, using the elevation of the surface of the impermeable layer in the mire depicted in (Fig. 7a). The initial conditions of this case were set as follows. Assuming the acrotelm of peat bogs, we established the initial thickness of the permeable layer to be 0.5 m and the spatial difference interval to be $\Delta x$ = 1.0 m. The time differential interval $\Delta t$ was calculated using Eq. (8) based on the water depth of the deepest pond at that time. We used the same PGF as depicted in Fig. 4, and we used repeatedly the observed rainfall time series for the Sarobetsu-mire. Other boundary conditions obtained using the above method adopted the following values:

Coefficients of permeability: $k_x$, $k_y$ = 0.005 m s$^{-1}$, roughness coefficient of Manning's formula: $n$ = 1.0, initial infiltration intensity: $f_O$ = 40.0 mm h$^{-1}$, final infiltration intensity: $f_c$ = 10.0 mm h$^{-1}$, time over which infiltration intensity declined by half: $a$ = 0.2 h, effective porosity: $\lambda_e$ = 0.2

The state of the slope 2000 years after the time at the start of the calculation, with the PGF defined as in Fig. 4 and the acceleration factor set to 50, is illustrated in Fig. 7b. The calculated ponds formed at nearly the same locations as the actual ponds, and the calculated pond depths were similar to those of the actual ponds. This result shows that the model simulated the mechanism of peat accumulation on the stair-like slope under the established boundary conditions. Even during the same period, the location and number of ponds would change if the amount and pattern of rainfall changed. The profile depicted in Fig. 7b is the result obtained for a hyetograph pattern reflecting light rainfall.

**Fig 8.** Concentric patterns on a lava plateau in Matsuyama-mire in Northern Hokkaido, Japan. (44°30´5.14´´N, 142°35´53.66´´E).

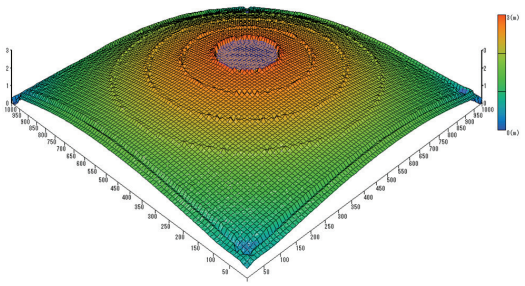

**Fig 9.** Simulated topographic pattern using the two-dimensional Carex model. The vertical scale is approximately 50 times greater than the horizontal distance.

### Example of the two-dimensional Carex model

The previous section provided an example of a one-dimensional calculation in which causalities are clearly elucidated; however, the model can also be applied to two-dimensional problems. An aerial view of the Matsuyama-mire in northern Hokkaido, Japan (44°30´5.14´´N, 142°35´53.66´´E) is presented in Fig. 8. This mire formed on a gently sloping lava plateau 800 m above sea level, created by volcanic activity in the Pleistocene Epoch of the Quaternary Period. Close inspection reveals a pattern of concentric circles in the gently sloping mire, which are sparse stands of dwarf Sakhalin spruce (*Picea glehnii*). It is known that this plant cannot grow if the water table is too shallow, and thus its presence is indicative of slightly drier environments. We considered that the observed pattern has been affected by water movement; therefore, we decided to apply the two-dimensional Carex model to this subject.

Assuming that wrinkles formed when the lava flow solidified, we placed concentric incline transition circles on the initial dome-like topography. We determined the constants of the boundary conditions as follows. The calculative matrix was 101 × 101, the spatial difference interval was 10 m, the initial thickness of the peat layer was 2.0 m, the coefficients of permeability in Darcy's law (i.e., $k_x$ and $k_y$) were both set at 0.1 cm s$^{-1}$, the roughness coefficient of Manning's formula was set at $n$ = 1.0, the initial infiltration intensity was set at $f_0$ = 40.0 mm h$^{-1}$, the final infiltration intensity was set at $f_c$ = 10.0 mm h$^{-1}$, the time over which the infiltration intensity declined by half was set at $\alpha$ = 0.2 h, and the effective porosity was set at $\lambda_e$ = 0.2. We used the PGF as depicted in Fig. 4, and used repeatedly the observed rainfall time series for the Sarobetsu-mire. The result of the calculation is presented in Fig. 9, which is drawn with a vertical scale that is approximately 50 times that of the horizontal distance. In mires with a shallow water table, peat accumulation is slightly greater at incline transition lines than in surrounding areas, and concentric small ridges form.

Additionally, a pond tends to form in the central flat part of the mire. Thus, the characteristics of a mire reflect the growth of trees in concentric circles on slightly drier ridges and the formation of a pond in the center of the mire where the groundwater is still and its level is high.

Causality in the two-dimensional model is more complex and various factors cause fluctuations in water flow. Okada (2009) reproduced the shape of bog rills using the two-dimensional model under an initial condition with highly permeable peat accumulated in an old river channel. Subsequently, Okada (2010) explained the formation processes of string-flark complexes, adding certain boundary conditions to the prototypical two-dimensional model.

## Discussion

### Interpretation of microtopography formation mechanism

In the study of the Kenashitai-mire on Mt. Hakkodasan, Yoshii and Hayashi (1935) noticed that

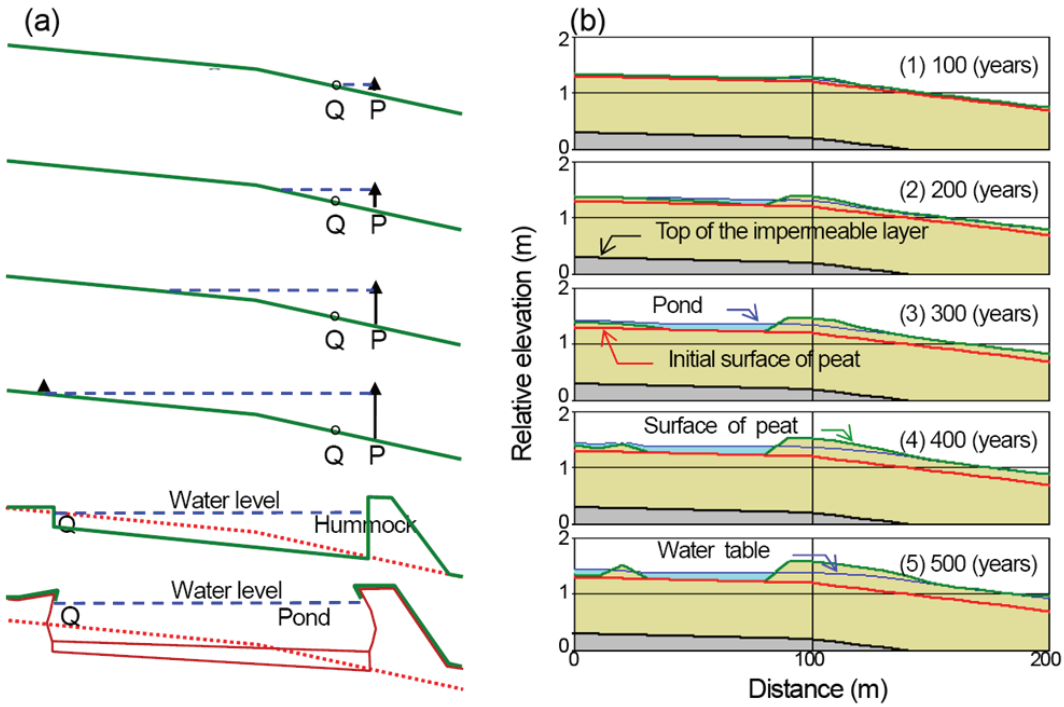


**Fig 10.** (**a**) Explanation of hollow formation by Yoshii and Hayashi (1935). Q: spring water point, P: plant growth point. Dashed blue line: water surface. Dotted red line: initial surface of peat. (**b**) Formation of a hollow (from the one-dimensional Carex model).

ridges often form on the downstream side of hollows of the sloping mire. The Kenashitai-mire is an oligotrophic mire on the western slope of the volcano Mt. Hakkodasan (40°39′52.35′′N, 140°51′43.95′′E). The mire is at an elevation of 1000-1200 m above sea level, and it forms a strip approximately 300 m wide and 1700 m long. After observing the above phenomenon in the many small ponds in the mire, Yoshii and Hayashi (1935) presented an explanation of the formation mechanism (Fig. 10a). They noted that springs tended to occur on the downstream side of the point of transition from a gentle to steep incline. They suggested that vigorous vegetation growth near spring locations would form peat ridges that would dam the upstream surface water flow. Consequently, wet ridges would accumulate more peat, deepening the water body and forming hollows. In Fig. 10a, Q marks the spring location, P indicates the location of plant growth, the dashed blue line represents the water surface, and the dotted red line identifies the initial surface of the peat.

Although Yoshii and Hayashi (1935) did not describe detailed boundary conditions, we specified topography similar to that depicted in Fig. 10a as the initial condition: a slope with inclination of 1/1000 changing to 1/200 downstream, permeable layer thickness of 1.0 m, and coefficient of permeability of 0.02 cm $s^{-1}$; other boundary conditions were the same as for the Naebayama-mire. The calculation results obtained under those conditions are shown in Fig. 10b. From the top to the bottom, the panels present the profile at 100-year intervals after the start of the calculation. In each panel, the lower red line marks the initial topography, the upper bold green line delineates the current topography, and the thin blue line shows the current water table.

At the incline transition point from a gentle to steep slope in the downstream direction, the water table is slightly below the ground surface of the initial topography. When the groundwater condition is in the aquatic wet range ([A] in Fig. 4), plants grow slightly better than in

**Fig 11.** Downslope pond formed at an incline transition point from a steep to gentle slope; Kyogoku- mire in Hokkaido, Japan (42°57′14.87′′N, 140°56′00.08′′E).

surrounding areas and extra peat accumulates, forming small ridges (Fig. 10b panel 1). Eventually, the upstream side of this ridge becomes wetter and grows at a rate smaller than that of the ridge itself (panel 2). As the ridge grows, the depth of the submerged area on the upstream side increases and a primitive hollow begins to form (panel 3). Because the properties of the peat mean that the hollow continues to supply water to the ridge body, the ridge continues to grow until it reaches equilibrium with the water table of the hollow (panel 4). Furthermore, because a secondary small incline transition point forms on the upstream side of the hollow, a secondary ridge occurs via the same process as that of the first ridge, and a secondary hollow begins to form (panel 5).

The concept of the PGF used in the Carex model differs slightly from that of Yoshii and Hayashi (1935) in the conditions established for maximum vegetation growth. However, because they are identical in that they consider the incline transition point as the trigger for hollow formation and both focus on the relationship with groundwater; the resulting shapes are very similar. The calculation results show that the lower slope of the ridge is slightly gentler than that presented by of Yoshii and Hayashi (1935) (Fig. 10a). This difference is believed to occur because the Carex model assumes that the peat properties are constant, whereas in reality those properties vary in a mire. It is known that the effective porosity and coefficients of permeability of a mire diminish with depth (e.g., Umeda 1981), further suggesting that peat properties change over time. Incorporating this variation in peat properties into the model is an issue that requires more detailed and quantitative knowledge, and must be addressed in the future.

In our study, a water table depth of +5 cm was set for the maximum vegetation growth position, and a water table depth of –5 cm was established as the limiting position of vegetation growth by the PGF. These positional relationships are important for the formation of the microtopography accompanied by the water surface, such as the formation of ridges, which dam the flow. In the theory of Yoshii and Hayashi (1935), a ridge forms on the downstream side of the incline transition point from a gentle to steep slope. However, in the Carex model, the incline transition point itself increases in height. On the basis of the PGF of the model, if there is spring water on the downstream side of the incline transition point from a gentle to a steep on the mire surface, the spring point will itself become a transition point to a gentle slope. An example of a small pond formed at the incline transition point from a steep to gentle slope can be found in Kyogoku-mire in Hokkaido, Japan (42°57′14.87′′N, 140°56′00.08′′E) (Fig. 11).

## Causality of one-dimensional model

In the model, the mechanism of pond formation on the slope can be considered as follows. On downslopes where the inclination changes from a gentle to steep slope, groundwater flow accelerates. This accelerated flow lowers the water table at the point of change in inclination. When the boundary condition is in range [A] (as in Fig. 4), i.e., a shallow water table, vegetation grows more vigorously at that point as the water table descends. Thus, over time, this point will grow as a hummock or ridge, eventually damming the water, and a pool will form on the upstream side of the hummock (Fig. 10b). However, if the boundary condition is in range [T] (as in Fig. 4), i.e., a deeper water table, vegetation growth at that point will be inhibited as the water table falls, preventing the formation of a pool.

In the model, bog microtopography is affected by differences in the water table caused

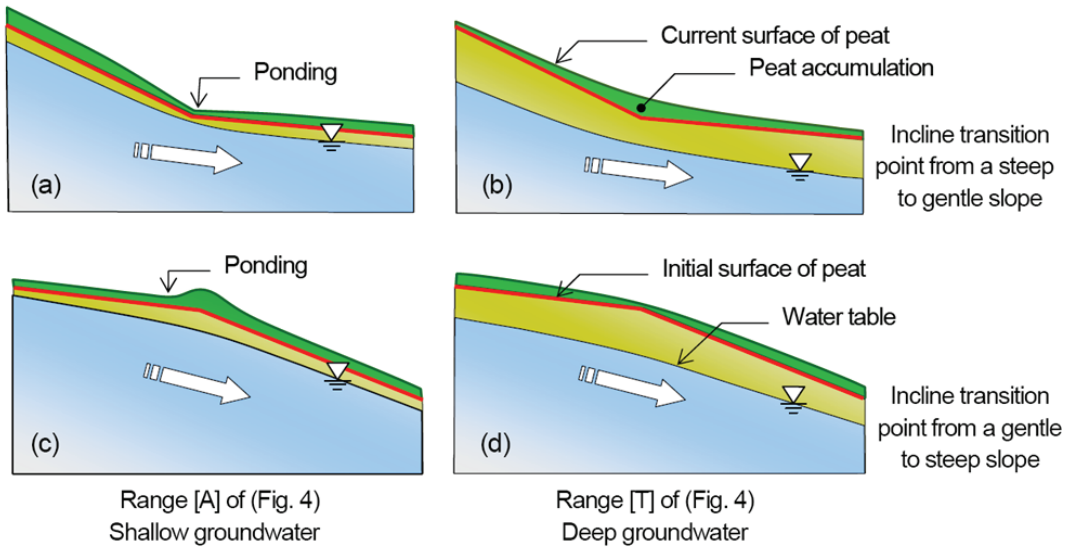


**Fig 12.** Schematics of peat accumulation around an incline transition point. Depending on common plant growth characteristics, ponds often form near the incline transition point on the bog surface. If the water table is shallow (**a**, **c**), a pond forms around the transition point. However, when the water table is deep (**b**, **d**), the incline transition point will be smoothed, no pond forms, and surface unevenness will become flattened.

by nonuniform groundwater flow. In the one-dimensional model used for the above examples, inequality of water flow under the initial conditions occurs only through a change in slope inclination. Thus, the causality is simple and clear in one-dimensional models. When the water table is high and low in the one-dimensional Carex model, differences in peat accumulation at the inclination change point are considered as follows.

Schematics of the differences in peat accumulation between the aquatic wet range ([A] as in Fig. 4) of the water table and the terrestrial dry range ([T] as in Fig. 4) are shown in Fig. 12. Profiles illustrating incline transition points from a steep to gentle slope in the downstream direction are shown in Fig. 12a and b, and profiles illustrating incline transition points from a gentle to steep slope in the downstream direction are shown in Fig. 12c and d. In both cases, the probability of pond formation increases only when the water table is shallow (left-hand diagrams). As mentioned in the previous section, at the transition point from a gentle to steep slope, a ridge forms at the point itself and a pond is formed by damming water upstream of the ridge (Fig. 12c). Conversely, at the point where the incline changes from a steep to gentle slope, the water table at the transition point becomes shallower than in the surrounding areas. Consequently, plant growth is suppressed only around the transition point and a depression is formed because of lesser peat accumulation; eventually, the depression becomes a pond (Figs. 12a and 11). Both cases demonstrate that a shallow water table is a common cause of pond formation.

## Potential of the Carex model

We believe that a simpler model mechanism is superior because it reveals causal relationships more clearly. In our study, the PGF is a nonlinear response function based only on the water table. Many studies have used the water table as a parameter that interacts with peat formation. For example, Swanson and Grigal (1988), Alexandrov (1988), Hilbert *et al*. (2000), Belyea and Clymo (2001), Couwenberg (2005), Couwenberg and Joosten (2005), and Harris *et al*. (2020) all described the relationship between peat accumulation and the water table. Among them, the relationship between the peat accumulation rate and the bog water level presented by Alexandrov (1988: fig. 3-2) closely resembles the PGF in

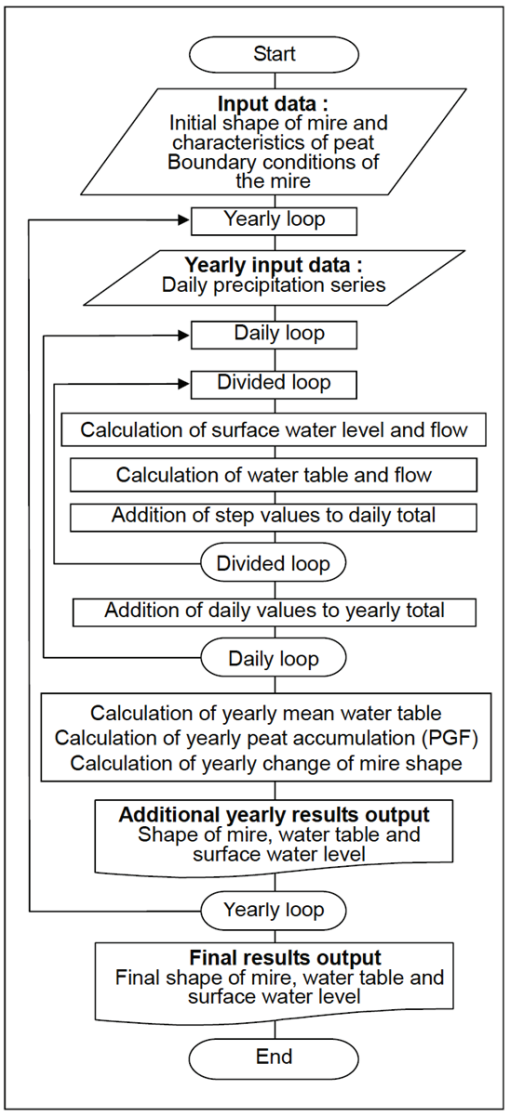


**Fig 13.** Calculation flowchart of the Carex model.

the Carex model. Moreover, the relationships presented by Belyea and Clymo (2001: fig. 2d), Nungesser (2003: fig. 9a), and Swanson (2007: fig. 1) are reasonably similar.

The Carex model simulates what occurs in existing mires. It can quantify and help visualize not only the changes in microtopographical shapes but also the water movements that cause them. If the calculated results differ from actual bog topography, the origin of the differences can be determined by examining the initial and boundary conditions. Repeated runs can bring the result of the computer simulation closer to the actual phenomenon. We believe that our study provides a solution that can clarify the process of formation of topographic patterns found in mires.

The two-dimensional Carex model can describe and reproduce the formation of typical microtopographies observed on mires (Okada 2009, Okada 2010, Okada 2013). In the model, the various factors can be set according to environmental conditions that vary regionally. By adding code to the prototype Carex model, we can represent the effect in which floating ice excavates the bottom of a pond during the snowmelt season. Additionally, we confirmed the potential of the model to perform reverse simulations going back into the past. In other words, it can trace back into the past and reproduce primitive topographic features by setting the present microtopographical shape as an initial condition and repeatedly subtracting the amount of peat growth estimated from the hydrological environment. Furthermore, when a mire development is planned, it is possible to predict the future impacts using the current shape and environments of the mire as the initial conditions and the changing boundary conditions.

Water movement on the surface and underground is influenced by meteorological conditions and the properties of the peat. The shape of the PGF (Fig. 4; Eq. 9) is based on the climate, peat properties, and ecological characteristics of the vegetation that dominate the area. Even in areas with similar meteorological and hydrological environments, the shape of the microtopographical patterns that form will vary if the dominant vegetation is different. We used the model with boundary conditions based on studies of mountain mires in the region of heavy snowfall in northern Japan. The Carex model is a flexible simulation model, and it can be applied to regions with different climates, peat characteristics, and vegetation if the boundary conditions such as vegetation growth characteristics and peat properties are set appropriately.

For readers with specific interest, a calculation flowchart of the Carex model is presented in Fig. 13, and we are prepared to provide a calculation program (Fortran) and a drawing program (VB-net) to anyone who would like to apply this model to their particular study area.

*Acknowledgements*: We are grateful to Professor Dr. Hiroko Fujita of Hokkaido University for providing genuine support and valuable advice. In particular, this paper would not have seen the light of day without the recommendation and encouragement of Prof. Richard A. Lindsay of the University of East London. We also thank Ms. Kaori Okada for her willingness to make calculations and provide effective translation. We thank James Buxton MSc, from Edanz (https://jp.edanz.com/ac), for editing a draft of this manuscript.

## References

Alexandrov, G. A. (1988). A spatially-distributed model of raised bog relief. In: *Wetland Modelling.Developments in Environmental Modelling* 12 (WJ Mitsch, M Straskraba, SE Jorgensen, Eds). Elsevier. pp. 41–53.

Belyea, L. R. and Clymo, R. S. (2001) Feedback control of the rate of peat accumulation. *Proc R Soc B* 268, 1315–1321.

Chow, V. T. (1959). Open channel hydraulics. McGrawHill

Couwenberg, J. (2005). A simulation model of mire patterning : revisited. *Ecography*, 28: 653–661.

Couwenberg, J., & Joosten, H. (2005). Self-organization in raised bog patterning : The origin of microtope zonation and mesotope diversity. *Journal of Ecology* 93: 1238–1248.

Eppinga, M. B., de Ruiter, P. C., Wassen, M. J., & Rietkerk, M. (2009). Nutrients and Hydrology Indicate the Driving Mechanisms of Peatland Surface Patterning. *The American Naturalist* 173: 804–818.

Fornberg, B. (1973). On the instability of leap-frog and Crank-Nicolson approximations of a nonlinear partial differential equation. *Mathematics of Computation* 2: 45–57.

Harris, L. I., Roulet, N. T. & Moore, T. R. (2020) Mechanisms for the Development of Microform Patterns in Peatlands of the Hudson Bay Lowland. *Ecosystems* 23, 741–767.

Hilbert, D. W., Roulet, N. & Moore, T. (2000) Modelling and analysis of peatlands as dynamical systems. *J Ecol* 88, 230–242.

Hirakawa, K. (2002). Geomorphological and Geological Examination on the Development of Uryunuma Mire in the Kabuto Mountains, Hokkaido, Japan. In: Tsujii, T. & Tachibana, H. (ed), *Wetlands of Hokkaido*, Maeda Ippoen Foundation, Akan. 163–169. (in Japanese)

Hogetsu, K., Ichimura, S., Hori, S., Oshima, Y., Kasanaga, H., Ono, H., & Takada, K. (1954). Phytoecological studies of Ozegahara Moor. In: Scientific Researchs of the Ozegahara Moor "Ozegahara". *Japan Society for the Promotion of Science* 313–400. (in Japanese with English abstract)

Hori, S. ,& Yajima, S. (1954). Ecological study on Naebayama mire. *Science reports of the Gumma University* 4 (5): 1–11. (in Esperanto with Japanese abstract)

Hori, S. (1961). Formation of Mire. Earth Science 55: 17-21. (in Japanese with Esperanto abstract)

Horton, R. E. (1940). Approach forward a physical interpretation of infiltration capacity. *Soil Science Society America* 5: 339–417.

Kito, N., & Hotes, S. (2014). Transition of bog vegetation and paleo environment. In: Fujita, H.(ed), Sarobetsu Mire and the Wakasakanai Coastal Dune Lakes and Forests, Hokkaido University Press, Sapporo 7–9. (in Japanese)

Lindsay, R. A. (2010). Peat bogs and carbon: A critical synthesis to inform policy development in oceanic peat bog conservation and restoration in the context of climate change. *Environmental Research Group*, University of East London, UK 304 pp. http://dspace.uel.ac.uk/jspui/handle/10552/1144

Nungesser, M. K. (2003). Modeling microtopography in boreal peat lands hummocks and hollows. *Ecological Modeling* 165: 175–207.

Okada, M. (2008). The Carex Model: Proposal for a microtopography formation model in bog mire using a vegetation growth function. Transactions, *Japanese Geomorphological Union* 29: 281–300. (in Japanese with English abstract) http://ci.nii.ac.jp/naid/110006862131

Okada, M. (2009). Formation of bog rills in Sarobetsu Mire: Verifying using Carex Model. Transactions, *Japanese Geomorphological Union* 30: 95–111. (in Japanese with English abstract) http://ci.nii.ac.jp/naid/110007227265

Okada, M. (2010). Formative process of string-flark (kermischlenke) complex pattern in boreal mires: Consideration based on the Carex Model. Transactions, *Japanese Geomorphological Union* 31: 17–32. (in Japanese with English abstract) http://ci.nii.ac.jp/naid/110007539550

Okada, M. (2013). Formation Process of Peat Islets in Bog Mire Ponds. Transactions, *Japanese Geomorphological Union* 34: 269–292. (in Japanese with English abstract) https://dl.ndl.go.jp/pid/10808743/1/1

Rietkerk, M., Dekker, S. C., Wassen, M. J., Verkroost, A. W. M., & Bierkens, M. F. P. (2004). A Putative Mechanism for Bog Patterning. The American Naturalist 163: 699–708.

Swanson, D. K., & Grigal, D. F. (1988). A simulation model of mire patterning. Oikos 53: 309–314.

Swanson, D. K. (2007). Interaction of mire microtopography, water supply, and peat accumulation in boreal mires. *Suo* 58(2): 37–47. Finnish Peatland Society .

Umeda, Y. (1981). Groundwater in peatland. Transition, *Japan Ground Water Technology Association* 23(6): 21–27. (in Japanese)

Whitaker, S. (1986). Flow in porous media I: A theoretical derivation of Darcy's law. *Transport in Porous Media* 1: 3–25.

Yoshii, Y., & Hayashi, N. (1935). Formation Process of Hakkoda Mire and the Study of "Ponds". *Ecology Research* 1(1): 1–14. (in Japanese)